Quantitative analyses of T cell motion in tissue reveals factors driving T cell search in tissues

David J Torres[1], Paulus Mrass[2], Janie Byrum[2], Arrick Gonzales[1], Dominick Martinez[1], Evelyn Juarez[1], Emily Thompson[3], Vaiva Vezys[3], Melanie E Moses[5], Judy L. Cannon[2,4]

[1] *Northern New Mexico College*
[2] *Department of Molecular Genetics and Microbiology, University of New Mexico School of Medicine*
[3] *Department of Microbiology and Immunology, University of Minnesota Medical School*
[4] *Autophagy, Inflammation, and Metabolism Center of Biomedical Research Excellence, University of New Mexico School of Medicine*
[5] *Department of Computer Science, University of New Mexico*

Abstract

T cells are required to clear infection, moving first in lymph nodes to interact with antigen bearing dendritic cells leading to activation. T cells then move to sites of infection to find and clear infection. T cell motion plays a role in how quickly a T cell finds its target, from initial naïve T cell activation by a dendritic cell to interaction with target cells in infected tissue. To better understand how different tissue environments might affect T cell motility, we compared multiple features of T cell motion including speed, persistence, turning angle, directionality, and confinement of motion from T cells moving in multiple tissues using tracks collected with two-photon microscopy from murine tissues. We analyzed naïve CD8 T cells moving within the lymph node with activated CD8 T cells moving within the villi of small intestine and lung under different activation conditions.

Our analysis found that while the speeds and the overall displacement of T cells vary within all tissues analyzed, T cells in all tissues tended to persist at the same speed, particularly if the previous speed is very slow (less than 2 μm/min) or very fast (greater than 8 μm/min). Interestingly, we found that turning angles of T cells in the lung show a marked population of T cells turning at close to 180°, while T cells in lymph nodes and villi do not exhibit this "reversing" movement. Additionally, T cells in the lung showed significantly decreased meandering ratios and increased confinement compared to T cells in lymph nodes and villi. The combination of these differences in motility patterns led to a decrease in the total volume scanned by T cells in lung compared to T cells in lymph node and villi. These results suggest that the tissue environment in which T cells move can impact the type of motility and ultimately, the efficiency of T cell search for target cells within specialized tissues such as the lung.

1 Introduction

Cell migration is a key feature of cellular function, and T cells are particularly specialized to migrate in different tissue types as infection can occur in any tissue and T cell movement in individual tissues is crucial to clear infection. Prior to infection, naïve CD8 T cells move within the paracortex of the lymph node, and upon interaction with cognate antigen bearing dendritic cells, T cells activate and effector CD8 T cells move to peripheral tissue sites of infection. In tissue sites, CD8 T cells enter infected tissues and move within tissues in order to find and kill target cells, including virally infected cells or tumor cells. While many studies have identified key molecules that regulate CD8 T cell effector function, still relatively little is known about how CD8 T cells navigate multiple different types of tissue environments to find target cells.

CD8 T cell motility is a key feature of CD8 T cell function, particularly in searching through complex tissue environments to identify and interact with target cells. Motility of T cells is a function of a combination of T cell-intrinsic mechanisms, the extracellular environment, and chemical signals in the milieu [27]. Tissue environments include a complex and heterogeneous system of cell types, extracellular matrix components, and soluble factors which have been shown to impact T cell motion; for example, structural cells within the tissue environment provide signals to feed back to immune cells in the central nervous system [7], [47]. Additionally, multiple studies have shown that naïve T cells in the lymph node paracortex use interactions with fibroblastic reticular cells to mediate movement, as well as receive soluble signals such as IL-7 for survival ([5], [26], [29]). In addition to extracellular influences, many studies have defined intrinsic molecular regulators of T cell movement, particularly speed in multiple tissues including lymph nodes ([19], [26], [21], [15], [13]), skin ([18], [17], [40] [3]), FRT [10] , liver ([22], [34], [43]), lung ([37], [2], [16]) just to name a few. High speeds have been linked to integrins (e.g. LFA-1 and VLA-4) [25] [40], chemokine receptors ([4], [39], [3]), as well as signaling molecules such as regulators of the actin cytoskeleton ([37], [30], [12]). These studies identified key molecular drivers and structures that mediate T cell movement within individual tissues, but there remains a gap in analysis to compare how T cell motility patterns might differ between tissues.

Quantitative analysis of cell motion provides a powerful tool to determine underlying mechanisms that drive how cells, including T cells, move. Studies performed both in vitro and in vivo have found that all cell movement, including T cells, use actomyosin contractility and actin flow to couple directional persistence and speed, pointing to a universal mechanism for cells to move faster and more persistently in a direction [24, 32]. This universal coupling of directional persistence and speed is most clearly shown in cells moving in vitro and on 2D surfaces. How T cells navigate complex tissue environments in three dimensions is still not well understood where cells use multiple modes of migration [50].

In this study, we quantitatively analyze T cell movement as one way to interrogate potential environment influences from different tissues. We previously used quantitative analyses of T cell movement in tissue to reveal specific types of motility patterns leading to more effective T cell responses (Fricke [19], Mrass [37], Thompson [46]). In this paper, we compare multiple features of T cell motion in different tissues: speed, tendency to persist at a speed, dependence of speed on turning angle, mean squared displacement, directionality, confined ratio and time, and volume patrolled within the lymph node with naïve CD8 T cells and activated CD8 T cells within the small intestine and lung. By comparing T cell movement in different tissues, we identify tissue specific effects on T cell motility. Our results suggest that tissue environments may contribute to different modes of T cell movement, which can impact the efficiency of T cell searches for target cells in tissues.

	Number of T cells	Type of T cell	Source
Lymph Node (LN)	5348	Naïve	Fricke [19] et al. and Tasnim et al. [45]
Small Intestine (villi)	828	Activated	Thompson et al. [46]
Lung (Flu)	99	Activated	Mrass and Cannon
Lung (LPS)	194	Activated	Mrass [37] et al.

Table 1. Two-photon microscopy T cell data

2 Materials and Methods

Table 1 summarizes the number of T cells tracked within the lymph node (LN), small intestine villi, and lung which were observed using two-photon microscopy. Cell tracks were obtained from at least 2 separate fields from at least 2 independent experiments. The data comes in the form of x-, y-, and z-coordinates for each T cell at different time frames. The lymph node T cell tracks were obtained from data in [19] and [45]. The T cell tracking in the small intestine was previously described in Thompson et al. [46]. T cells from LPS inflamed lung were previously described [37].

For T cells from influenza infected lung, mice were infected intranasally with a 1×10^3 PFU HKx31 (Charles River). To ensure sedimentation of the virus into the lower respiratory tract, infection was performed while mice were under anesthesia with 90 mg/kg ketamine and 8.1mg/kg xylazine. In some experiments mice received polyclonal naïve GFP+CD8+ T cells from Ubiquitin-GFP animals before infection with influenza. GFP+CD8+ naive T cells were derived from single cell suspensions isolated from spleen and lymph nodes of Ubiquitin GFP animals, and CD8+ T cells isolated using the CD8a+ T Cell Isolation Kit (Miltenyi Biotec), then transferred via the tail vein into recipient mice. Recipient mice received approximately 10^4 GFP+CD8+ T cells. All work was done in accordance with approved protocols per IACUC institutional approvals.

For imaging of GFP+CD8+ T cells in influenza infected lungs, lungs from influenza infected mice were removed at days 7 or 8 post infection, then mice were euthanized and after opening the chest cavity, the lungs were inflated with 2% low melting agarose (Sigma-Aldrich, A0701) at a temperature of 37 degrees. We injected one ml of the solution via a catheter through an incision of the trachea. After inflation, the opening in the trachea was sealed with a knot and agarose solidification was induced by exposing the lungs to a PBS solution with a temperature of 4 degrees Celsius. After harvest the lungs were transferred into an incubator and transferred within a biosafety cabinet into a POC-R imaging chamber (LaCon). Imaging was performed with a Zeiss LSM800 Airyscan Confocal Microscope. Due to the transparency of the prepared lung tissue, it was possible to visualize at tissue depths of more than 60 µm. In some experiments, imaging was performed with similar setups using a Prairie Ultima Two-photon microscope or a Zeiss LSM 510 microscope. We captured equivalent T cell behavior with the different microscope setups.

Below we summarize the time step sampling and the various metrics used to analyze the T cell motion. These metrics include speed (cell-based speed and displacement speed), tendency to persist at the same speed, mean squared displacement, directionality through the meandering ratio, confined ratio and time, and volume patrolled.

2.1 Sampling

Due to the different time steps used in the two-photon microscopy of the different tissues, we sample the position data every 90 seconds (or as close to 90 seconds as possible) for each of the tissues to normalize and equalize T cell analyses. Also, we are able to use all the data for results involving the turning angle by revisiting times that are skipped in an initial 90 second sampling. For example, suppose observations are made at the following times $\{t_0, t_1, t_2, t_3, t_4, ...\}$ where $t_0 = 0\ s$, $t_1 = 45\ s$, $t_2 = 90\ s$, $t_3 = 135\ s$, $t_4 = 180\ s$ and so on. The first sampling of the data retains $\{t_0, t_2, t_4, ...\}$ and the second sampling uses $\{t_1, t_3, t_5, ...\}$. We do not sub-sample the LPS-inflamed lung data since the time steps are initially 90 seconds. After this sampling is done, the lymph node mean time step was 89.9 seconds with a standard deviation of 2.9 seconds, the villi mean time step was 93.0 seconds with a standard deviation of 7.9 seconds, the lung (flu) mean time step was 90.0 seconds with a standard deviation of 0.12 seconds, and the lung (LPS) mean time step was 90.0 seconds with a standard deviation of 0.10 seconds.

2.2 Speed

If (x_i, y_i, z_i) refers to the position of the cell at time t_i and $(x_{i+1}, y_{i+1}, z_{i+1})$ refers to the position of the cell at time t_{i+1}, let $d_{i,i+1}$ represent the distance between the two positions

$$d_{i,i+1} = \sqrt{(x_{i+1} - x_i)^2 + (y_{i+1} - y_i)^2 + (z_{i+1} - z_i)^2}. \tag{1}$$

Two different types of speeds are computed using the positions and times from a T cell: a cell-based speed and displacement-based speed.

2.2.1 Cell-based speed

If a cell is tracked for n positions and times, the average speed s_{cell} of a cell is computed by summing all the distances traveled by the cell and dividing by the total elapsed time $t_n - t_1$,

$$s_{cell} = \frac{\sum_{i=1}^{n-1} d_{i,i+1}}{t_n - t_1}. \tag{2}$$

2.2.2 Displacement-based speed

The displacement-based speed is computed using the first and last locations of the cell,

$$s_{displacement} = \frac{d_{1,n}}{t_n - t_1}. \tag{3}$$

2.3 Turning angle and directionality

The turning angle θ for a T cell given the three positions of the cell {1,2,3} enclosed within circles is shown in the left image below. If $\mathbf{v}_1$ is the vector formed from positions (x_1, y_1, z_1) and (x_2, y_2, z_2), $\mathbf{v}_1 = (x_2 - x_1, y_2 - y_1, z_2 - z_1)$ and $\mathbf{v}_2$ is the vector formed from positions (x_2, y_2, z_2) and (x_3, y_3, z_3),
$\mathbf{v}_2 = (x_3 - x_2, y_3 - y_2, z_3 - z_2)$, the turning angle θ is computed using

$$\theta = arccos\left(\frac{\mathbf{v}_2 \cdot \mathbf{v}_1}{||\mathbf{v}_1||||\mathbf{v}_2||}\right). \tag{4}$$

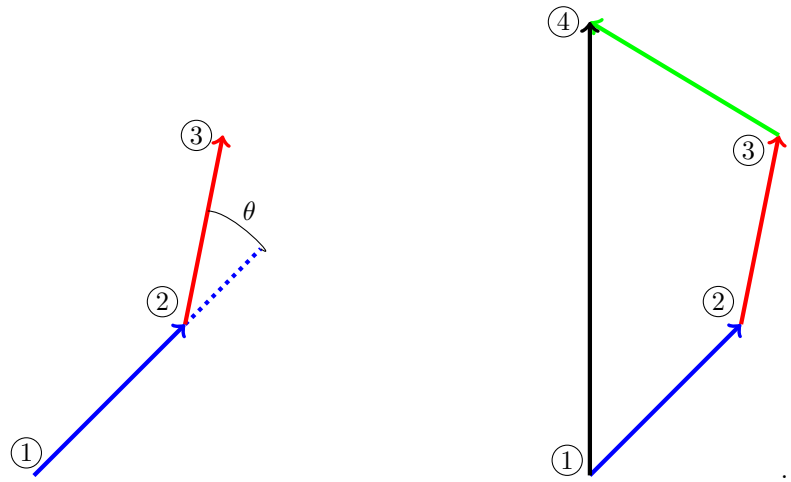

We did not include speeds less than 1 μm/min as these cells are likely to be considered stopped and turning angles with very small speeds can lead to artifactual angle measurements; for example, small speeds will emphasize turning angles in increments of 45° degrees due to the pixel resolution of the microscope.

Suppose a T cell visits the four locations enclosed within the circles as shown in the right image above. One can compute the total distance travelled by summing up the distance from location 1 to location 2, $d_{1,2}$, the distance from location 2 to location 3, $d_{2,3}$, and the distance from location 3 to location 4, $d_{3,4}$. The straight line distance can also be computed from the original location 1 to the final location 4, $d_{1,4}$. One measure of a cell's tendency to maintain its direction is the meandering ratio [16]

$$M = \frac{d_{1,4}}{d_{1,2} + d_{2,3} + d_{3,4}}.$$

If the ratio M is close to 1, the cell deviates very little from one direction, whereas if M is much less than 1, the cell moves along a meandering path. In general for n locations, directionality can be measured using the ratio

$$M = \frac{d_{1,n}}{\sum_{i=1}^{n-1} d_{i,i+1}}. \tag{5}$$

2.4 Confined ratio and confined time

We denote the amount of time a T cell lingers in one location as confined time. Given a time t_i and location (x_i, y_i, z_i), we count the time difference between t_i and $t_j > t_i$ as confined time if the difference $t_j - t_i$ is greater than 150 seconds and the distance $d_{i,j}$ is less then 5 μm. Once the cell exits (say at time t_k) the 5 μm radius centered about (x_i, y_i, z_i), the cell is tracked anew and the confined time is computed from t_k and location (x_k, y_k, z_k). We call the ratio of confined time to the total time the confined ratio.

In regards to confined time, we calculate the amount of time required to leave a 5 μm radius for each cell position. The time is then averaged over all positions to find the confined time.

2.5 Tendency to persist at a speed

Let s_b and s_a be two consecutive frame speeds (before and after) in μm per minute from a T cell track. If B_i represents the event that s_b lies between i μm per minute

and $(i+1)$ μm per minute, then the probability of event B_i occurring is $P(B_i) = m_b/m$, where m_b represents the number of times i μm/min $\leqslant s_b < (i+1)$ μm/min and m represents the total number of tracks. If A_i represents the event that i μm/min $\leqslant s_a < (i+1)$ μm/min, then the probability $P(A_i) = m_a/m$ where m_a represents the number of times i μm/min $\leqslant s_a < (i+1)$ μm/min. Finally it follows that $P(A_i \; and \; B_i) = m_{ab}/m$ where m_{ab} represents the number of times both criteria are satisfied: i $\mu m/min \leqslant s_a, s_b < (i+1)$ $\mu m/min$ in consecutive frames. According to the definition of conditional probability $P(A_i|B_i) = P(A_i \; and \; B_i)/P(B_i) = m_{ab}/m_b$. The increased probability of persisting at the same speed is then calculated as the ratio $P(A_i|B_i)/P(A_i) = (m \cdot m_{ab})/(m_a \cdot m_b)$.

2.6 Mean squared displacement

Values of the log of the mean squared displacement (MSD) are plotted against the log of the elapsed time. We limit the elapsed time to 10.5 minutes. The slope of the linear regression line is computed from the scatter plot and used to characterize the type of motion. Slope values less than 1.0 are associated with Brownian motion, values between 1.0 and 2.0 are associated with Lévy walks, and values less than 1.0 are considered subdiffusive [27].

2.7 Rate of volume patrolled

The volume patrolled by a T cell is computed by dividing a 400 μm x 400 μm x 400 μm volume within which a T cell moves into 2.5 μm x 2.5 μm x 2.5 μm cubes. If the distance between a cube center and the T cell center is less than 5 μm, the cube volume is assumed to be patrolled. We also connect each two successive cell positions with a straight line and assume the cell patrols volume along the straight line. The total volume patrolled is then divided by the time the T cell is tracked.

3 Results

3.1 Speed

We began our analysis with a comparison of the cell-based average speeds of T cells in multiple tissues including naïve CD4 and CD8 T cells in the lymph node (LN) in the absence of infection [19]("LN"); effector CD8 T cells moving in the villi in response to LCMV infection at d8 post infection [46]("Villi"); effector CD8 T cells moving in LPS inflamed lung at d7-8 post infection [37](Lung LPS); and effector CD8 T cells in influenza-infected lung at d7-8 post infection (Lung Flu). We previously found no difference in motility speed and patterns of naïve CD4 and CD8 T cells in lymph nodes [19]. To ensure consistency across analyses, we normalized time steps to 90 seconds for all datasets (for details, see Data and Methods). Figure 2A and Figure 2B shows the box-and-whisker plot of cell-based speed and displacement speed from each tissue.

The median cell-based speed for naive T cells in the LN was 6.2 μm/min, CD8 effector T cells in the villi 4.6 μm/min, CD8 effector T cells from influenza infected lung (Flu) 5.2 μm/min and CD8 effector T cells from LPS-inflamed lung (LPS) 4.3 μm/min. Pairwise p-values based on cell-based average speeds from two different tissues are reported in Table 2. P-values are computed using the paired Wilcoxon Rank Sum test (otherwise known as the Mann-Whitney test) using the statistical package R with the Bonferroni correction for multiple comparisons. We found that naïve T cells in lymph nodes moved faster than effector CD8 T cells in both the gut villi and lung. Between lung and villi, effector CD8 T cells in the influenza-infected

lung moved slightly faster than effector CD8 T cells in the villi of the small intestine (Fig. 2A: lung (Flu) 5.2 μm/min vs villi 4.6 μm/min ($p = 5.3 \times 10^{-10}$)) or LPS-inflamed lung (Fig. 2A: lung (Flu) 5.2 μm/min vs lung (LPS) 4.3 μm/min ($p = 4.9 \times 10^{-5}$)). Effector CD8 T cells in gut villi moved at similar speeds to effector CD8 T cells in LPS inflamed lung but the difference was still statistically significant. Supplemental Figure 1A shows the frequency distribution of speeds for T cells moving in each tissue type, with T cells from lymph nodes and influenza-infected lung showing more cells moving at higher speeds than T cells in villi or LPS-inflamed lung (S1A). T cells in either influenza-infected lung or LPS-inflamed lung also have a large proportion of cells moving at slower speeds than T cells in lymph nodes or villi, with T cells in LPS-inflamed lung showing the largest proportion of cells moving at slow speeds. These results suggest that the specific tissue environment does not appear to dictate speed of T cell movement.

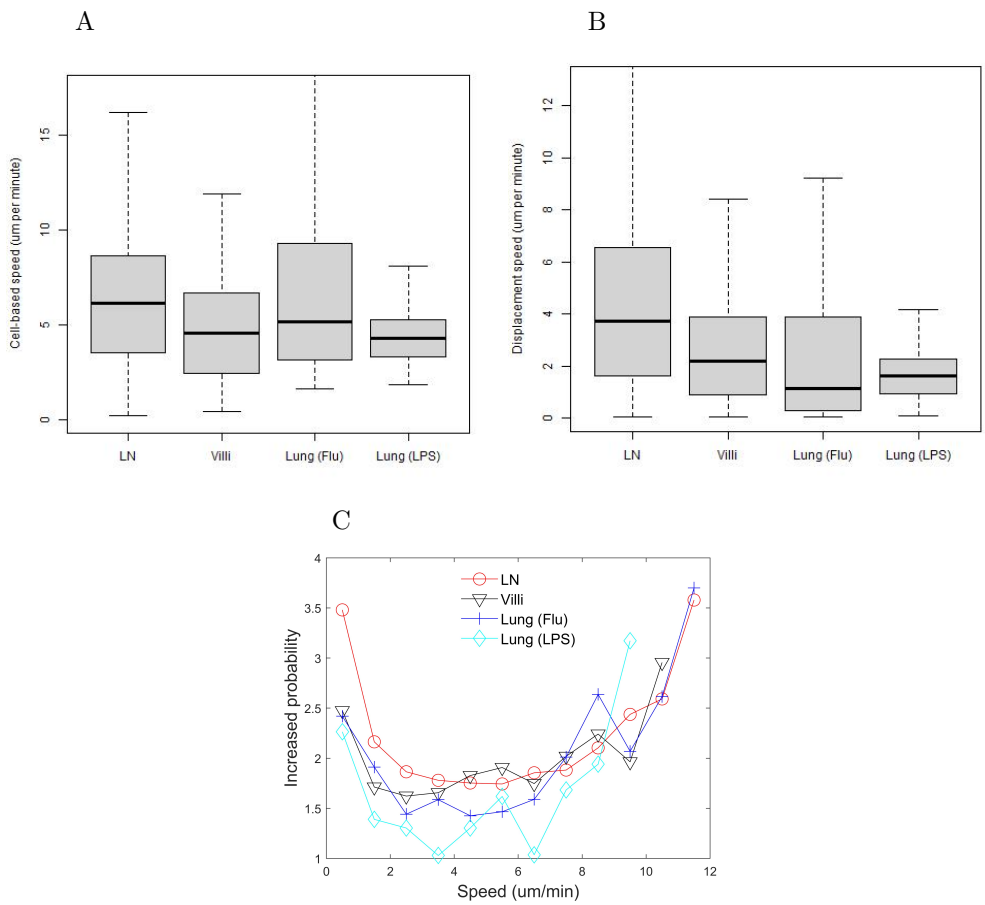

Fig 2. Speed distribution of T cells does not correlate with tissue type but T cell moving in the lung show less persistence. (A) Box-and-whisker plot of cell-based speed (μm/min) of T cells moving in LN (median 6.2), villi (median 4.6), lung (Flu infected) (median 5.2) and lung (LPS) (median 4.3). (B) Box-and-whisker plot of displacement speed (μm/min) of T cells in lymph (median 3.7), villi (median 2.1), lung (Flu infected) (median 1.1) and lung (LPS instilled) (median 1.6). (C) Distribution plot of probability to persist at the same speed.

We then calculated displacement speed of T cells in each tissue, which measures the speed at which the cell moves away from an initial location and is smaller than the

	LN	Villi	Lung (Flu)	Lung (LPS)
LN	1.0	$< 2 \times 10^{-16}$	1.0	5.4×10^{-14}
Villi	$< 2 \times 10^{-16}$	1.0	5.3×10^{-10}	1.0
Lung (Flu)	1.0	5.3×10^{-10}	1.0	4.9×10^{-5}
Lung (LPS)	5.4×10^{-14}	1.0	4.9×10^{-5}	1.0

Table 2. Table of p-values of pairwise comparisons of cell-based speed as shown in Figure 2A using Wilcoxon rank sum test.

	LN	Villi	Lung (Flu)	Lung (LPS)
LN	1.0	$< 2 \times 10^{-16}$	$< 2 \times 10^{-16}$	$< 2 \times 10^{-16}$
Villi	$< 2 \times 10^{-16}$	1.0	1.3×10^{-7}	6.6×10^{-4}
Lung (Flu)	$< 2 \times 10^{-16}$	1.3×10^{-7}	1.0	0.13
Lung (LPS)	$< 2 \times 10^{-16}$	6.6×10^{-4}	0.13	1.0

Table 3. Table of p-values of pairwise comparisons of displacement speed shown in Figure 2B using Wilcoxon rank sum test.

cell-based speed in all the tissues (Figure 2B). The displacement speed is highest in naïve T cells in LN (median 3.7 μm/min) followed by effector CD8 T cells within the villi (2.1 μm/min). In the lung, effector CD8 T cells within the LPS-inflamed lung (1.6 μm/min) moved at speeds slightly higher to cells in the influenza-infected lung (1.1 μm/min, $p = 0.13$). P-values of comparisons between each T cell type are reported in Table 3. We found that the displacement speed of effector CD8 T cells in the lung in both influenza infection and LPS treatment are both statistically significantly lower than T cells in the villi (villi 2.1 μm/min and influenza-infected lung 1.1 μm/min, $p = 1.3 \times 10^{-7}$; villi and LPS lung 1.6 μm/min, $p = 6.6 \times 10^{-4}$). There was no statistical difference between displacement speed of CD8 effector T cells in the influenza-infected lung or LPS-inflamed lung (influenza-infected lung 1.1 μm/min, and LPS lung 1.6 μm/min, $p = 0.13$). Supplemental Figure 1B shows the frequency distrubtion of T cell displacement speed ((S1B). These results suggest that the lung environment leads to lower displacement speed of T cells.

3.2 Persistence

The difference between cell-based speed (Fig. 2A) and displacement speed particularly of CD8 effector T cells in influenza infected lung (Fig. 2B) suggests that the likelihood of persisting at a specific speed may be different in the lung. We calculated the likelihood that an individual T cell will persist in moving at the same speed in each tissue (Figure 2C). We quantified the probability that a T cell will continue to move at the same speed as the previous time step and termed this "persistence" (for detailed methods, see Section 2.5). For example, if a cell moves at greater than 10 μm/min, we calculated the likelihood that the same cell will continue to persist at the same speed in subsequent time steps.

We observed a similar trend to persist at very high and very low speeds for T cells moving in all tissues observed. Similar likelihood of persistence in speed was exhibited at very low speeds (< 2 μm/min), with naive T cells in the lymph node showing

higher likelihood of stopping than T cells in other tissues. While all T cells showed the highest persistence at very low and very high speeds, Fig 2C showed that in general, T cells in the lung showed lower persistence probability than T cells in the lymph node or villi, especially at intermediate speeds (between $3-7$ μm/min). These data suggest that the lung environment may hinder the ability of T cells to move persistently.

3.3 Mean squared displacement

We then determined the mean squared displacement (MSD) of each T cell moving in each tissue. (Fig. 3A) shows the median T cell track for a T cell from each tissue type. We determined the linear regression line through a scatter plot of the log of the MSD speed versus time for each T cell in (Fig. 3A). We then calculated the slope of the MSD for all the T cells from each tissue by plotting log of the mean squared displacement speed versus the log of elapsed time for all T cells within each tissue within each tissue (Fig. 3B). T cells are tracked for a maximum of 10.5 minutes to ensure consistency of analysis across tissues. [27].

As shown in Fig. 3B, T cell motion in the LN and villi could be characterized as superdiffusive with values >1. In contrast, the slope of T cells in the LPS inflamed lung was close to one (0.94) while the slope of T cells in the influenza infected lung is less than one (0.88) (Fig. 3B). The p-values comparing the differences between the mean square displacement slopes of T cells moving in individual tissues are shown in Table 4. While there were statistical differences between the other tissues, there was less statistical difference between the MSD slopes between T cells in the influenza infected and LPS inflamed lung ($p = 0.096$). These results show that T cells moving in the lung do not show superdiffusive behavior seen in LNs and villi.

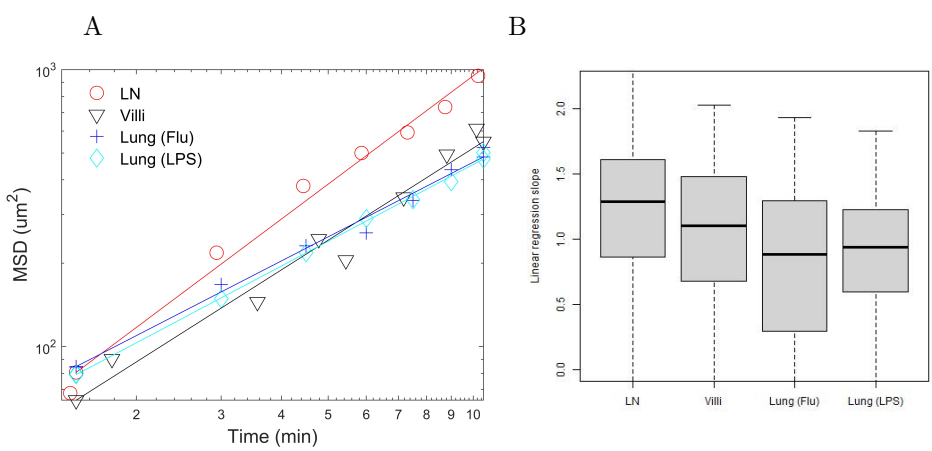

Fig 3. (A) Plots of mean square displacement (MSD) vs time and least squares lines of individual representative cells near median from Fig. 3B. (B) Box-and-whisker plots of log transformed least square cell slopes of mean squared displacement vs time. The median values are LN (1.3), villi (1.1), lung (Flu) (0.88), and lung (LPS) (0.94).

3.4 Turning angle and dependence of speed on turning angle

As persistence in cell motion is related to turning angles, we analyzed the turning angles of T cells in individual tissues. Figure 4A plots the relative frequency of all turning angles of T cells moving in different tissues. We did not include T cells moving at speeds less than 1 μm/min. We reasoned that turning angles are not relevant when a cell is moving very slowly (< 1 μm/min). Also small speeds will emphasize turning

	LN	Villi	Lung (Flu)	Lung (LPS)
LN	1.0	5.0×10^{-15}	$< 2.0 \times 10^{-16}$	1.8×10^{-15}
Villi	5.0×10^{-13}	1.0	1.7×10^{-10}	6.8×10^{-4}
Lung (Flu)	$< 2.0 \times 10^{-16}$	1.7×10^{-10}	1.0	9.6×10^{-2}
Lung (LPS)	1.8×10^{-15}	6.8×10^{-4}	9.6×10^{-2}	1.0

Table 4. Table showing mean square displacement P-values as pairwise comparisons from Figure 3 using Wilcoxon rank sum test.

angles in increments of 45° degrees due to the pixel resolution of the microscope. Since the distribution is not uniform, the cell motion cannot be considered Brownian.

We found that while T cells in all tissues show some preference for turning angles between $40^o - 50^o$, many more T cells in the lymph node and villi showed this preference to turn at smaller angles compared to T cells in the lung. In fact, T cells moving in the lung showed a peak at approximately 160°, a behavior not seen in T cells moving in lymph node and villi. While the difference between the turning angle distributions between T cells in all tissues is significant by statistical comparison (p-values are shown in Table 5.), the pattern of turning angles between CD8+ effector T cell in the lung both show fewer T cells moving between $40^o - 50^o$ and more T cells showing the peak at 160°. This peak is likely due to the "back and forth" motion observed in T cells in the lung which we have previously described [37]. The higher percentage of T cells turning at smaller angles in the lymph nodes and villi suggests that these organs allow a broader range of turning motion, potentially enabling broader search areas.

We extended our analysis by determining if there exists a relationship between speed and the turning angle. Maiuri et al. [32] and Jerison and Quake [24] previously found that T cells that move faster generally move persistently in one direction and show a small turning angle while slower T cells show higher turning angles. Our results confirmed that T cells in lymph node, villi, and influenza-infected lung moving with faster speeds exhibit smaller turning angles while T cells moving with slower speeds exhibit larger turning angles for all tissues (Figure 4B). Interestingly, effector CD8 T cells moving in the LPS-inflamed lung did not show the speed-turning angle correlation (Figure 4B, cyan), suggesting that the relationship between speed and turning angle may not be universal. The behavior in the LPS lung could be due to the fact that T cells in the LPS-inflamed lung have a slow cell-based speed; however, the flatness of the line suggests that even slow T cells in LPS-inflamed lung may not be subject to the same mechanisms that regulate the speed-angle behavior seen in faster moving cells. We also note that T cells in the influenza-infected lung and LPS-inflamed lung experience a small increase in speeds for turning angles between 160° and 180°.

3.5 Directionality and Confinement

The combination of persistence and turning angle determines the directionality of cell movement. The fact that displacement speed is lower than the cell-averaged speed suggests that persistence in T cell movement may differ in the different tissues analyzed. We assessed directionality by calculating a "meandering ratio" which quantified how likely a T cell deviates from its original direction. Figure 5 shows the box-and-whisker plot of the meandering ratio of T cells moving within the different tissues. T cells in the lymph node and villi move significantly more directionally than

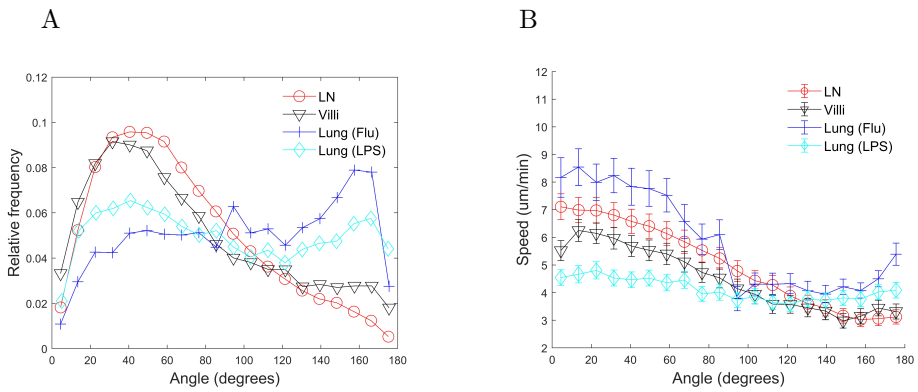

Fig 4. Turning angles and coupling of speed and turning angles of T cells in different tissues. (A) Relative frequency distribution of turning angles in each tissue. T cells moving in the lung show a peak at approximately 160°. (B) Plot of speed (um/minute) versus angle (degrees). The speed tends to decrease as the turning angle increases in all tissues except for T cells in the LPS-inflamed lung. Error bars show plus and minus 1/8 of the standard deviation within each 9° angle bin.

	LN	Villi	Lung (Flu)	Lung (LPS)
LN	1.0	1.1×10^{-12}	$< 2.0 \times 10^{-16}$	$< 2.0 \times 10^{-16}$
Villi	1.1×10^{-12}	1.0	$< 2.0 \times 10^{-16}$	2.1×10^{-9}
Lung (Flu)	$< 2.0 \times 10^{-16}$	$< 2.0 \times 10^{-16}$	1.0	2.6×10^{-3}
Lung (LPS)	$< 2.0 \times 10^{-16}$	2.1×10^{-9}	2.6×10^{-3}	1.0

Table 5. Table of p-values of pairwise comparisons of proportion of turning angles less than 90° shown in Figure 4A using Wilcoxon rank sum test.

T cells in the lung (median values for the meandering ratio are lymph node: 0.70, villi: 0.53, lung (Flu): 0.22, and lung (LPS): 0.37.). Pairwise p-value comparisons are reported in Table 6.

We have previously shown that T cells can alternate between confined motion in which the search area is localized and ballistic motion in which motion is fast and persistent in a direction [37]. We calculated the confined ratio as defined by the time a T cell spends confined versus moving in Figure 6A. We found that naïve T cells in the lymph node spend very little time confined and most of the time moving, showing a median confined ratio of 0.15. Effector CD8 T cells in both the villi and influenza infected lung show similar confined ratios of 0.53 while effector T cells in LPS-inflamed lung showed the highest confined ratio of 0.60. We also calculated the average amount of time T cells from each tissue spend confined which is reported as confined time in Figure 6B. We found that T cells in the lung and villi showed significantly longer confined times than T cells in lymph node with T cells in LPS-inflamed lung showing the longest time spent confined. For the exact definition of confined ratio and confined time see Section 2.4. P-values are reported in Table 7 and Table 8. These data show that effector CD8 T cells in LPS-inflamed lung were most confined followed by T cells in influenza-infected lung (Flu) and T cells in the villi. Naive T cells in the lymph node were the least confined. These data suggest that the lymph node environment with the least confinement is likely to contribute to the high meandering ratio of T

cells while confinement as well as antigen in tissues such as lung and gut likely decrease the ability of T cells to meander in tissues (5).

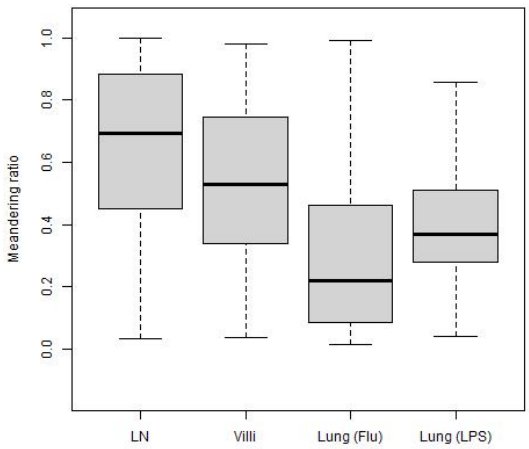

Fig 5. Meandering ratio within different tissues. The median values are LN (0.70), villi (0.53), lung (Flu) (0.22), and lung (LPS) (0.37).

	LN	Villi	Lung (Flu)	Lung (LPS)
LN	1.0	$< 2 \times 10^{-16}$	$< 2 \times 10^{-16}$	$< 2 \times 10^{-16}$
Villi	$< 2 \times 10^{-16}$	1.0	$< 2 \times 10^{-16}$	8.7×10^{-13}
Lung (Flu)	$< 2 \times 10^{-16}$	$< 2 \times 10^{-16}$	1.0	4.3×10^{-9}
Lung (LPS)	$< 2 \times 10^{-16}$	8.7×10^{-13}	4.3×10^{-9}	1.0

Table 6. Table shows p-values of pairwise comparisons of meandering ratio as shown in Figure 5 using Wilcoxon rank sum test.

	LN	Villi	Lung (Flu)	Lung (LPS)
LN	1.0	$< 2 \times 10^{-16}$	$< 2 \times 10^{-16}$	$< 2 \times 10^{-16}$
Villi	$< 2 \times 10^{-16}$	1.0	0.52	0.29
Lung (Flu)	$< 2 \times 10^{-16}$	0.52	1.0	1.8×10^{-2}
Lung (LPS)	$< 2 \times 10^{-16}$	0.29	1.8×10^{-2}	1.0

Table 7. Table showing p-values of pairwise comparisons of confined ratios from Figure 6A using Wilcoxon rank sum test.

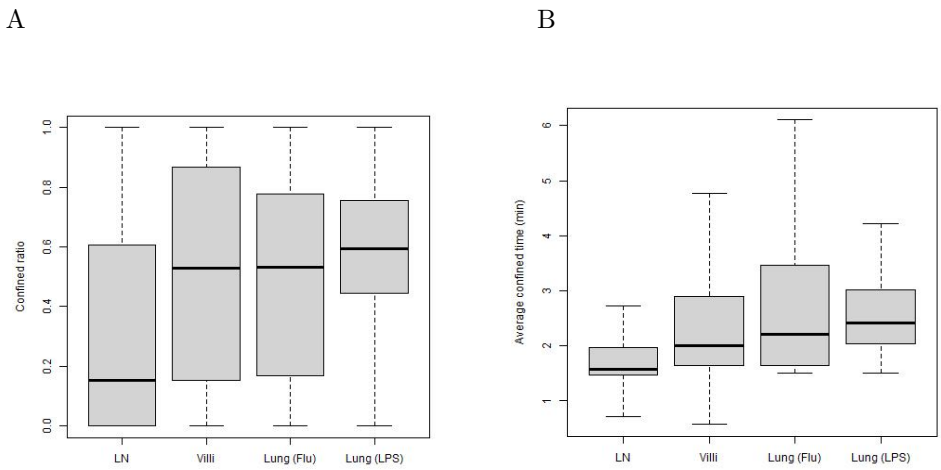

Fig 6. Confinement of T cells from different tissues. (A) Box-and-whisker plot of confined ratios. Median values: LN 0.15, Villi 0.53, Lung (Flu) 0.53, Lung (LPS) 0.60. (B) Box-and-whisker plot of confined time. Median values (min): LN 1.6, Villi 2.0, Lung (Flu) 2.2, Lung (LPS) 2.4.

	LN	Villi	Lung (Flu)	Lung (LPS)
LN	1.0	$< 2 \times 10^{-16}$	$< 2 \times 10^{-16}$	$< 2 \times 10^{-16}$
Villi	$< 2 \times 10^{-16}$	1.0	1.0	1.3×10^{-6}
Lung (Flu)	$< 2 \times 10^{-16}$	1.0	1.0	5.4×10^{-2}
Lung (LPS)	$< 2 \times 10^{-16}$	1.3×10^{-6}	5.4×10^{-2}	1.0

Table 8. Table showing p-values of pairwise comparisons of confined time from Figure 6B using Wilcoxon rank sum test.

3.6 Patrolled volume per time

A key function of T cell movement is surveillance of tissues. To assess whether differences we identified in cell speed, directionality, turning angle, and confined ratio ultimately translate into differences in the ability of T cells to survey tissue, we calculated the volume per time patrolled by a T cell residing in different tissues taking into account all the different motility parameters we have previously identified. Figure 7A shows the amount of volume per time patrolled by the T cells in individual tissues taking into account each of the motility parameters we previously defined. The volume surveyed is highest for naïve T cells in lymph node (median 9.4 μm^3/s) and intermediate for CD8 effector T cells in villi (6.5 μm^3/s). Effector CD8 T cells in the lung showed the lowest volume patrolled: the volume patrolled by T cells in the influenza-infected lung (5.3 μm^3/s) was statistically similar to the volume patrolled by T cells in the LPS-inflamed lung (5.1 μm^3/s). See Table 9 for the p-values.

We also analyzed the full distribution of volume patrolled by T cells in each individual tissue (Figure 7B). The full distribution showed that T cells in lymph nodes show the largest volume patrolled per time, T cells in the villi show an intermediate volume, with fewer T cells at the low volumes (<5 μm^3/s) but also fewer T cells

patrolling large volumes (>15 μm^3/s). Interestingly, although the median patrolled volume is similar, T cells in influenza-infected lung actually show a large number of cells patrolling at both low and large volumes. The Kolmogorov-Smirnov test compares the distributions and shows statistically significant differences in all pairwise comparisons (Table 10). T cells in LPS-inflamed lung mostly show low patrol volumes as expected. These data demonstrate that the combination of speed, turning angles, directional movement, and confinement times all contribute to the ability of T cells to search tissue environments for potential targets.

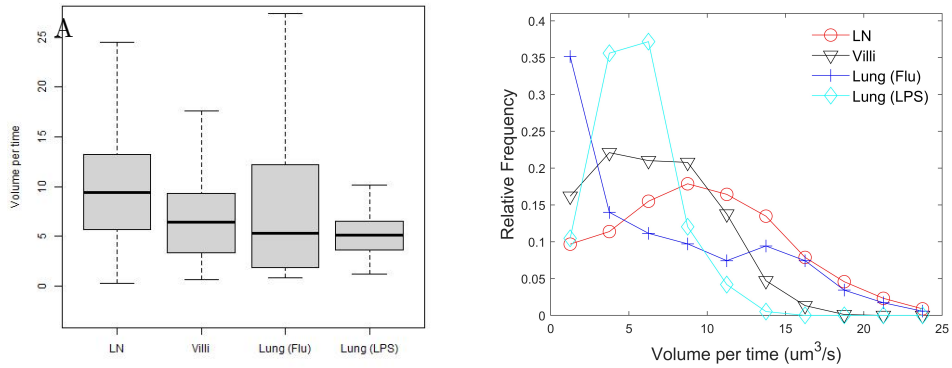

Fig 7. Volume patrolled by T cells in different tissues. (A) Box-and-whisker plot of median volume per time (cubic microns per second) patrolled by T cells in LN (9.4), villi (6.5), lung (flu) (5.3), and lung (LPS) (5.1). (B) Relative frequency distribution of volume per time (cubic microns per second) patrolled by T cells in each tissue.

	LN	Villi	Lung (Flu)	Lung (LPS)
LN	1.0	$< 2 \times 10^{-16}$	$< 2 \times 10^{-16}$	$< 2 \times 10^{-16}$
Villi	$< 2 \times 10^{-16}$	1.0	1.0	4.4×10^{-4}
Lung (Flu)	$< 2 \times 10^{-16}$	1.0	1.0	1.0
Lung (LPS)	$< 2 \times 10^{-16}$	4.4×10^{-4}	1.0	1.0

Table 9. Table of p-values of pairwise comparisons of volume per time from Figure 7A using Wilcoxon rank sum test.

4 Discussion

Cell movement through tissue is an important feature in immunity, particularly for T cell mediated immunity as T cells must make direct cell-cell contact with target cells. We analyzed motility parameters to determine what key factors drive the ability of T cells to move through tissues to effectively mount immune responses. Using data from naïve T cells moving in lymph nodes and effector CD8 T cells moving in gut villi and lung, we identified similarities and differences that contribute to the ability of T cells to search tissue for target cells. We found that T cell speed all fall within a similar

	LN	Villi	Lung (Flu)	Lung (LPS)
LN	1.0	$< 1.3 \times 10^{-15}$	$< 1.3 \times 10^{-15}$	$< 1.3 \times 10^{-15}$
Villi	$< 1.3 \times 10^{-15}$	1.0	2.0×10^{-8}	1.6×10^{-8}
Lung (Flu)	$< 1.3 \times 10^{-15}$	2.0×10^{-8}	1.0	2.2×10^{-8}
Lung (LPS)	$< 1.3 \times 10^{-15}$	1.6×10^{-8}	2.2×10^{-8}	1.0

Table 10. Table of p-values of pairwise comparisons of volume per time distributions from Figure 7B using Kolmogorov-Smirnov test.

range regardless of the differentiation state of T cells, but that naïve T cells patrol a larger volume due to a combination of fast speed, less confinement, more super-diffusive motion, and smaller turning angles. In contrast, while effector T cells in the lung upon influenza infection can move at fast speeds comparable to naive T cell speed, the patrol volume is significantly smaller for effector T cells in the influenza-infected lung due to greater confinement, more Brownian-like motion, and a greater proportion of large turning angles, particularly angles that suggest a "back and forth" motion. Our analysis more fully captures the key features of movement that enable T cells to effectively move in tissues, promoting T cell responses.

Our analysis included naïve CD8 and CD4 T cells in the lymph node, antigen specific effector CD8 T cells responding to infection in the villi and lung (influenza-infected lung), and non-antigen specifically activated effector CD8 T cells in the LPS-inflamed lung in a model of acute lung injury [37]. Interestingly, speed analysis shows that T cells tend to persist at a similar range of speeds in all tissue types regardless of activation status with non-antigen specific naïve T cells moving fastest in lymph nodes and effector CD8 T cells moving the slowest in the LPS-inflamed lung when comparing cell-based speed. Cell-based speed also did not correlate with tissue type, with effector CD8 T cells in the lung capable of moving faster (as in influenza-infected lung) or slower (as in LPS-inflamed lung). However, the displacement speed did correlate well with mean squared displacement. These data suggest that the speed at which T cells move can be independent of antigen specific interactions as well as activation status. These results are supported by previous work showing that effector CD8 T cells in the skin appear to move slowly [3] while effector CD8 T cells in the female reproductive tract move at speeds similar to naïve T cells in lymph nodes [10].

Previous work quantitating cell motility in both non-T cells as well as T cells observed a "universal coupling" between speed and directional persistence, showing that fast moving cells show directional persistence while slow moving cells do not [32][24]. In our analysis, we find that T cells moving in lymph node, small intestine villi, and influenza-infected lung all show this coupling. However, we have also identified an exception to this rule for T cells moving in the LPS-inflamed lung, which showed no change in persistence as measured by turning angle between fast moving and slow moving cells (Figure 4B). Recently, it has been shown that the correlation between speed and turning angle can arise from differences in sampling rates [20]. Our data is unlikely to be affected by sampling rate as we equalized and normalized the sampling rate for all the T cells (see Data and Methods). Thus, while our data confirm that while speed can be coupled to directional persistence for T cells moving in all tissues analyzed, this coupling is not necessarily "universal".

We find that T cells moving in the lung show specific motility features that differ from T cells moving in lymph nodes or villi. T cells in the lung tend to displace less,

turn at higher angles, particularly at angles > 140°, meander more, and linger at locations longer. Confinement can occur in the lung independent of antigen, as CD8 T cells activated in vitro in the LPS-inflamed lung can still show confinement without specific antigen activation. In particular, T cells in the lung exhibit back and forth motion, with a peak of turning angles near 160°. This peak in turning angle is consistent with the "back and forth" motion we previously observed for T cells in the LPS-inflamed lung, as well as a stop-and-go motion [37]. Stop-and-go behavior has also been observed albeit for shorter time periods for T cells in lymph nodes by Miller et al. [35], Wei et al. [49], and Beltman et al. [8]. We also find that the slope of the MSD vs time for T cells moving in lymph nodes and villi show super-diffusive motion as previously observed for effector T cells in the brain [23]. In contrast, the slope of T cells moving in lung is slightly less than 1, suggesting Brownian type motion. However, because the angle distribution is not uniform, the cell motion cannot be considered strictly Brownian. Together these motility parameters suggest that the lung environment may lead to a specific types of motion taken by T cells, potentially due to the particular physical environment of the lung.

The volume patrolled by a T cell is dependent not only on its speed but also on turning angles, the cell's tendency to meander, and the amount of time the cell spends confined to a location. The higher percentage of T cells turning at smaller angles in the lymph nodes and villi suggests that these organs allow a broader range of turning motion, potentially enabling broader search areas as reflected in the larger volumes patrolled. The naïve T cells in the lymph nodes move with the highest speed, lower turning angles, and lowest confinement time, and thus naïve T cells in lymph nodes show the highest volume covered per second (9.4 um^3/sec). However, T cells in the lung are similar to T cells in villi for patrol volume despite having significantly less directional motion and more confinement. However, T cells in the influenza-infected lung and LPS-inflamed lung show differences in the frequency of T cells patrolling, with T cells in the influenza-infected lung showing more T cells patrolling at higher volumes than T cells in LPS-inflamed lung or T cells in the villi. These results suggest that a combination of back and forth motion and slightly faster speeds can make up for improved search efficiency for T cells in the influenza-infected lung. Previous results using computational modeling suggests that intermittent and back-and-forth motion can improve search times [9]. Effector T cells moving in LPS-infected lung show the lowest volume covered (5.1 um^3/s) due to low speeds, higher turning angles, low directionality and high confinement times. The lack of coupling between speed and turning angle may also lead to low search efficiency.

Three-dimensional migration of T cells is a complex interplay of the internal cell signaling, surrounding extracellular tissue environment, and molecular signaling and cytokines. We have quantitatively analyzed how T cells move in different tissues using multiple metrics. These metrics provide a way of quantitatively capturing underlying complex features of three-dimensional T cell movement.

5 Funding

This work was supported by an Institutional Development Award (IDeA) from the National Institute of General Medical Sciences of the National Institutes of Health under Grant P20GM103451.(DJT); NIH 1R01AI097202 (JLC), the Spatiotemporal Modeling Center (P50 GM085273), the Center for Evolution and Theoretical Immunology 5P20GM103452 (JLC), AIM CoBRE at UNM HSC NIH P20GM121176 (JLC; PM), NIH 5 T32 AI007538-19 (JRB), institutional support from dedicated health research funds from UNM SOM (JLC), Women in Science Award from UNM, DARPA/AFRL FA8650-18-C-6898 (JLC) and in part institutional support from

Dedicated Health Research Funds from the UNM School of Medicine (JLC and PM); and support by the University of New Mexico Comprehensive Cancer Center Support Grant NCI P30CA118100 (JLC and PM).

References

1. Allenspach EJ, Cullinan P, Tong J, Tang Q, Tesciuba AG, Cannon JL, et al. ERM-dependent movement of CD43 defines a novel protein complex distal to the immunological synapse. Immunity. Elsevier; 2001;15: 739-750. doi: 10.1016/s1074-7613(01)00224-2

2. Alon R, Sportiello M, Kozlovski S, Kumar A, Reilly EC, Zarbock A, Garbi N, Topham DJ. Leukocyte trafficking to the lungs and beyond: lessons from influenza for COVID-19. Nat Rev Immunol. 2021; 21(1):49-64. doi: 10.1038/s41577-020-00470-2.

3. Ariotti S, Beltman JB, Borsje R, Hoekstra ME, Halford WP, Haanen J, de Boer RJ, Schumacher TNM. Subtle CXCR3-dependent chemotaxis of CTLs within infected tissue allows efficient target localization. J Immunol. 2015; 195(11): 5285-95. doi: 10.4049/jimmunol.1500853.

4. Asperti-Boursin F, Real E, Bismuth G, Trautmann A, Donnadieu E. CCR7 ligands control basal T cell motility within lymph node slices in a phosphoinositide 3-kinase-independent manner. Journal of Experimental Medicine. 2007; 204(5): 1167-1179. doi 10.1084/jem.20062079.

5. Bajenoff M, et al. Stromal cell networks regulate lymphocyte entry, migration, and territoriality in lymph nodes. Immunity. 2006; 25:989–1001. doi: 10.1016/j.immuni.2006.10.011

6. Banigan EJ, Harris TH, Christian DA, Hunter CA, Liu AJ. Heterogeneous CD8+ T cell migration in the lymph node in the absence of inflammation revealed by quantitative migration analysis. PLoS Comput Biol. 2015; 11(2):e1004058. https://doi.org/10.1371/journal.pcbi.1004058

7. Bartholomaus I, et al. Effector T cell interactions with meningeal vascular structures in nascent autoimmune CNS lesions. Nature. 2009; 462: 94-98. https://doi.org/10.1038/nature08478

8. Beltman JB, Maree AFM, Lynch JN, Miller MJ, de Boer RJ. Lymph node topology dictates T cell migration behavior. Journal of Experimental Medicine. 2007; 204(4): 771. https://doi.org/10.1084/jem.20061278

9. Bénichou O, Loverdo C, Moreau M, Voituriez R. Intermittent search strategies. Reviews of Modern Physics. 2011; 83: 81-129. doi: 10.1103/RevModPhys.83.81

10. Beura LK, et al. Intravital mucosal imaging of CD8+ resident memory T cells shows tissue-autonomous recall responses that amplify secondary memory. Nat Immunol. 2018; 19(2): 173-182. doi: 10.1038/s41590-017-0029-3.

11. Bousso P, Bhakta NR, Lewis RS, Robey E. Dynamics of thymocyte-stromal cell interactions visualized by two-photon microscopy. Science. 2002; 296: 1876-80. pmid:12052962 doi: 10.1126/science.1070945

12. Cannon JL, Asperti-Boursin F, Letendre KA, Brown IK, Korzekwa KE, Blaine KM, et al. PKCθ regulates T cell motility via Ezrin-Radixin-Moesin localization to the uropod. PLoS One. 2013; 8: e78940. pmid:24250818. https://doi.org/10.1371/journal.pone.0078940

13. Devi S, Alexandre YO, Loi JK, Gillis R, Ghazanfari N, Creed SJ, Holz LE, Shackleford D, Mackay LK, Heath WR, Sloan EK, Mueller SN. Adrenergic regulation of the vasculature impairs leukocyte interstitial migration and suppresses immune responses. Immunity. 2021; 54(6): 1219-1230 doi: 10.1016/j.immuni.2021.03.025.

14. Donovan GM, Lythe G. T-cell movement on the reticular network. J Theor Biol. 2012; 295: 59-67. doi: 10.1016/j.jtbi.2011.11.001.

15. Eckert N, Permanyer M, Yu K, Werth K, Förster R. Chemokines and other mediators in the development and functional organization of lymph nodes. Immunological Reviews. 2019; 289(1): 62-83. doi: 10.1111/imr.12746.

16. Emo KL, Hyun Y-M, Reilly E, Barilla C, Gerber S, Fowell D, Kim M, Topham DJ. Live imaging of influenza infection of the trachea reveals dynamic regulation of CD8+ T cell motility by antigen. PLoS Pathogens. 2016; 12(9): e1005881. doi: 10.1371/journal.ppat.1005881

17. Fernandes NRJ, Reilly NS, Schrock DC, Hocking DC, Oakes PW, Fowell DJ. CD4+ T cell Interstitial Migration Controlled by Fibronectin in the Inflamed Skin. Front. Immunol. 2020; 11: 1501. doi: 10.3389/fimmu.2020.01501.

18. Fowell DJ, Kim M. The spatio-temporal control of effector T cell migration. Nat Rev Immunol. 2021; 21(9): 582-596. doi: 10.1038/s41577-021-00507-0.

19. Fricke GM, Letendre KA, Moses ME, Cannon JL. Persistence and adaptation in immunity: T cells balance the extent and thoroughness of search. PLoS Comput Biol. 2016; 12(3): e1004818. doi:10.1371/journal.pcbi.1004818.

20. Ganusov VV, Zenkov VS, Majumder B. Correlation between speed and turning naturally arises for sparsely sampled cell movements. bioRxiv https://www.biorxiv.org/content/10.1101/2020.12.30.424897v5

21. Gérard A, Patino-Lopez G, Beemiller P, Nambiar R, Ben-Aissa K, Liu Y, Totah FJ, Tyska MJ, Shaw S, Krummel, MF. Detection of rare antigen-presenting cells through cell-intrinsic meandering motility, mediated by Myo1g. Cell. 2014; 158(3): 492-505. doi: 10.1016/j.cell.2014.05.044.

22. Guidotti LG, et al. Immunosurveillance of the liver by intravascular effector CD8(+) T cells. Cell. 2015; 161(3): 486-500. doi: 10.1016/j.cell.2015.03.005.

23. Harris TH, Banigan EJ, Christian DA, Konradt C, Wojno EDT, Norose K, et al. Generalized Lévy walks and the role of chemokines in migration of effector CD8+ T cells. Nature. 2012; 486: 545-548. pmid: 22722867 doi: 10.1038/nature11098

24. Jerison ER, Quake SR. Heterogeneous T cell motility behaviors emerge from a coupling between speed and turning in vivo. eLife. 2020; 9:e53933 doi: 10.7554/eLife.53933.

25. Katakai T, Habiro K, Kinashi T. Dendritic cells regulate high-speed interstitial T cell migration in the lymph node via LFA-1/ICAM-1. J Immunol. 2013; 191:1188–99. doi: 10.4049/jimmunol.1300739

26. Katakai T, Hara T, Sugai M, Gonda H, Shimizu A. Lymph node fibroblastic reticular cells construct the stromal reticulum via contact with lymphocytes. J Exp Med. 2004; 200:783–95. doi: 10.1084/jem.20040254

27. Krummel MF, Bartumeus F, Gérard A. T cell migration, search strategies and mechanisms. Nat Rev Immunol. 2016; 16(3): 193-201. https://doi.org/10.1038/nri.2015.16

28. Letendre K, Asperti-Boursin F, Donnadieu E, Moses ME, Cannon JL. Bringing statistics up to speed with data in analysis of lymphocyte motility. PLoS One. 2015; 10(5): e0126333. https://doi.org/10.1371/journal.pone.0126333

29. Link, A., et al. Fibroblastic reticular cells in lymph nodes regulate the homeostasis of naive T cells. Nat Immunol. 2007; 8(11): 1255-65. https://doi.org/10.1038/ni1513

30. Nombela-Arrieta C, Mempel TR, Soriano SF, Mazo I, Wymann MP, Hirsch E, Martínez-A C, Fukui Y, von Andrian UH, Stein JV. A central role for DOCK2 during interstitial lymphocyte motility and sphingosine-1-phosphate-mediated egress. J Exp Med. 2007; 204(3): 497-510. doi: 10.1084/jem.20061780.

31. Onder, L., et al. IL-7-producing stromal cells are critical for lymph node remodeling. Blood. 2012; 120(24): 4675-83. doi: 10.1182/blood-2012-03-416859

32. Maiuri P, Rupprecht JF, Wieser S, Ruprecht V, Bénichou O, Carpi N, et al. Actin flows mediate a universal coupling between cell speed and cell persistence. Cell. 2015; 161(2): 374-386. doi: 10.1016/j.cell.2015.01.056

33. Matheu MP, Parker I, Cahalan MD. Dissection and 2-photon imaging of peripheral lymph nodes in mice. J Vis Exp JoVE. MyJoVE Corporation 2007; doi: 10.3791/265

34. McNamara HA, et al. Up-regulation of LFA-1 allows liver-resident memory T cells to patrol and remain in the hepatic sinusoids. Sci Immunol. 2017; 2(9). doi: 10.1126/sciimmunol.aaj1996.

35. Miller MJ, Wei SH, Cahalan MD, Parker I. Autonomous T cell trafficking examined in vivo with intravital two-photon microscopy. Proc Natl Acad Sci. 2003; 100(5): 2604-2609. https://doi.org/10.1073/pnas.2628040100 https://doi.org/10.1073/pnas.2628040100

36. Miller MJ, Hejazi AS, Wei SH, Cahalan MD, Parker I. T cell repertoire scanning is promoted by dynamic dendritic cell behavior and random T cell motility in the lymph node. Proc Natl Acad Sci. 2004; 101: 998-1003. https://doi.org/10.1073/pnas.0306407101

37. Mrass P, Oruganti SR, Fricke GM, Tafoya J, Byrum JR, Yang L, Hamilton SL, Miller MJ, Moses ME, Cannon JL. ROCK regulates the intermittent mode of interstitial T cell migration in inflamed lungs. Nature Communications. 2017; 8(1): 1010 doi: 10.1038/s41467-107-01032-2.

38. Obenaus M, Leitão C, Leisegang M, Chen X, Gavvovidis I, van der Bruggen P, Uckert W, Schendel DJ, Blankenstein T. Identification of human T-cell receptors with optimal affinity to cancer antigens using antigen-negative humanized mice. Nature Biotechnology. 2015; 33(4) doi: 10.1038/nbt.3147.

39. Okada T, Cyster JG. CC chemokine receptor 7 contributes to Gi-dependent T cell motility in the lymph node. J Immunol. 2007; 178(5): 2973-8. doi: 10.4049/jimmunol.178.5.2973.

40. Overstreet, MG, et al. Inflammation-induced interstitial migration of effector CD4+ T cells is dependent on integrin αV. Nat Immunol. 2013; 14(9): 949-58. doi: 10.1038/ni.2682.

41. Petrie RJ, Yamada KM. At the leading edge of three-dimensional cell migration. Journal of Cell Science. 2012; 125(24): 5917-5926. doi: 10.1242/jcs.093732

42. Preston SP, Waters SL, Jensen OE, Heaton PR, Pritchard DI. T-cell motility in the early stages of the immune response modeled as a random walk amongst targets. Phys Rev E Stat Nonlin Soft Matter Phys. 2006; 74(1) doi: 10.1103/PhysRevE.74.011910.

43. Rajakaruna H, O'Connor JH, Cockburn IA, Ganusov VV. Liver Environment-Imposed Constraints Diversify Movement Strategies of Liver-Localized CD8 T Cells. J Immunol. 2022; 208(5): 1292-1304. doi: 10.4049/jimmunol.2100842.

44. Renner K, Bruss C, Färber S. (n.d.). Monitoring human T cell activation in the context of immunotherapeutic approaches. OLS OMNI Life Science GmbH & Co KG.

45. Tasmin H, Fricke GM, Byrum JR, Sotiris JO, Cannon JL, Moses ME. Quantitative measurement of naïve T cell association with dendritic cells, FRCS, and blood vessels in lymph nodes. Frontiers in Immunology. 2018; 9:1571. doi: 10.3389/fimmu.2018.01571

46. Thompson EA, Mitchell JS, Beura LK, Torres DJ, Mrass P, Pierson MJ, Cannon JL, Masopust D, Fife BT, Vezys V. Interstitial Migration of CD8$\alpha\beta$ T cells in the small intestine is dynamic and is dictated by environmental cues. Cell Reports. 2019; 26: 2859-2867 doi.org/10.1016/j.celrep.2019.02.034.

47. Tomlin H, Piccinini AM. A complex interplay between the extracellular matrix and the immune response to microbial pathogens. 2018; 155(2): 186-201. doi: 10.1111/imm.12972

48. Vezys V, Yates A, Casey KA, Lanier G, Ahmed R, Antia R, Masopust D. Memory CD8 T-cell compartment grows in size with immunological experience. Nature. 2009; 457(7226): 196-199. doi: 10.1038/nature07486

49. Wei SH, Parker I, Miller MJ, Cahalan MD. A stochastic view of lymphocyte motility and trafficking within the lymph node. Immunol Rev. 2003; 195: 136-159. doi: 10.1034/j.1600-065x.2003.00076.x

50. Yamada KM, Sixt M. Mechanisms of 3D cell migration. Nat Rev Mol Cell Biol. 2019; 20: 738-752. https://doi.org/10.1038/s41580-019-0172-9

Appendix A Supplementary material

Figures S1A and S1B show the distribution of cell-based and displacement-based speeds respectively.

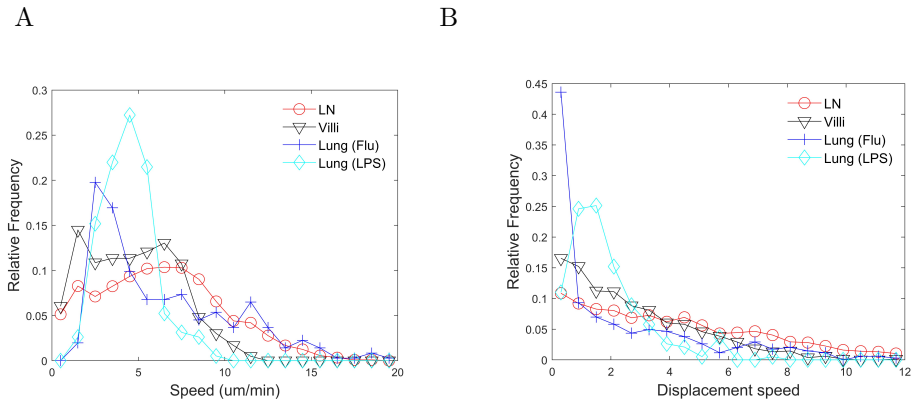

Fig S1. (A) Relative frequency distribution of T cell speed in lymph, villi, lung (Flu activated) and lung (LPS activated). The distributions use the average cell-based speed of each T cell. (B) Relative frequency distribution of T cell displacement speed in lymph, villi, lung (Flu activated) and lung (LPS activated). The distributions use the displacement speed of each T cell.